9 Methods for Determination of Enzyme Kinetics and Metabolic Rates

MURALI SUBRAMANIAN

Pharmaceutical Candidate Optimization, Biocon Bristol-Myers Squibb Research Center, Syngene International Ltd, Bangalore, India

TIMOTHY S. TRACY

Department of Pharmaceutical Sciences, College of Pharmacy, University of Kentucky, Lexington, KY, USA

9.1 SUMMARY

Determination of the *in vitro* kinetics of metabolism of drugs is critical to the drug discovery and development process. This typically involves using some type of enzyme system (e.g., human liver microsomes, expressed enzymes, and hepatocytes) to measure metabolite formation rates and enzyme involvement (reaction phenotyping). For most compounds, this process usually follows the Michaelis–Menten type of enzyme kinetics resulting in a hyperbolic rate of metabolite formation. However, for some compounds, an atypical kinetic profile may be observed, for example, sigmoidal, biphasic, or substrate inhibition kinetics. Regardless, the proper kinetic equation must be used to describe the kinetics and obtain the most accurate kinetic parameters. These estimated parameters are then used for *in vitro–in vivo* correlation (IVIVC) analyses to predict the human *in vivo* pharmacokinetics and the doses to be used in phase I clinical trials.

Encyclopedia of Drug Metabolism and Interactions, 6-Volume Set, First Edition.
Edited by Alexander V. Lyubimov.

9.2 BACKGROUND

The introduction of a new chemical entity to the market is a long and expensive process with many potential pitfalls [1]. An integral component of drug discovery and development is determination of the enzymes catalyzing metabolism of the drug, the kinetics involved therein, and the resulting metabolic products. Previously, most of these efforts were focused on the cytochrome P450 (P450 or CYP) enzymes, the primary enzymes involved in oxidative metabolism. However, as drug discovery efforts were focused on reducing P450-mediated metabolism, other enzyme families such as the glucuronosyl transferases (UGTs), the sulfotransferases (SULTs), the flavin monooxygenases (FMOs), gained importance, resulting in efforts to determine of the kinetics of these enzymatic reactions, as well. The kinetics of metabolizing enzyme reactions contributes to the half-life of a drug and its elimination rate, thus affecting the dosing regimen and potentially the route of administration. In addition, the resulting metabolic products are not always inactive or innocuous, potentially resulting in toxicity or other adverse effects. Thus, the proper identification of the enzymes involved in metabolism of a drug, the resulting metabolic products, and the kinetics of these processes is paramount to successful drug development.

This chapter summarizes the current state of knowledge in enzyme kinetics, including both typical and atypical enzyme kinetics. Also included is a discussion of the various *in vitro* systems employed to determine enzyme kinetic rates and the resulting products, as well as the strengths and weaknesses of each system. Finally, methods of determining kinetics with the intent of estimating *in vivo* clearances are discussed, as are the basics of enzyme inhibition.

9.3 *IN VITRO* SYSTEMS TO STUDY ENZYME KINETICS

There are three well-established systems to study P450 kinetics (microsomes, hepatocytes, and expressed enzymes), as well as a newly developed cell line, HepaRG, that is being tested for suitability to study drug-metabolizing enzyme kinetics. Each of these systems offers unique advantages and disadvantages for conducting *in vitro* determinations of enzyme involvement and kinetics of reactions. In fact, one usually employs a complement of the various systems to maximize the information gained, while optimizing the use of resources and reducing overall time to derive the desired information.

9.3.1 Human Liver Microsomes (HLMs)

The most commonly used system for determining drug-metabolizing enzyme kinetics are human liver microsomes (HLMs), prepared from human livers. In this case, the endoplasmic reticulum fraction is isolated from human liver tissue, typically obtained from tissue that was deemed nontransplantable. This system retains all the P450s as well as other microsomal enzymes such as the UGTs and FMOs [2]. Obviously, microsomes may be prepared from any animal species, permitting study of metabolism in that species. HLMs are relatively easy to prepare, convenient to use, can be stored frozen (-80°C) for long periods of time with little relative loss of activity, and are comparatively less expensive than other systems. Because they can be prepared in

relatively large quantities and then stored frozen, the same "batch" can be used for an extended period of time, allowing direct comparison of results conducted over time. It is relatively common for investigators to create a "master mix" of HLMs, pooled from multiple donors. Frequently, proportions of HLMs from various donor livers, wherein the relatively activity of various P450 enzymes has been characterized are mixed to create a "master mix" with known isoform activity levels assumed to be representative of the population at large (in contrast to representing only a single individual). These pooled HLMs also avoid the potential use of a prep from an individual liver that might be deficient in metabolism by a particular isoform due to genetic polymorphisms that might provide misleading results.

HLMs offer additional advantages, including the fact that the enzymes are also anchored in the lipid membranes as they would be anchored in the liver *in vivo*. With respect to the P450s, HLMs also contain the redox partners cytochrome P450 reductase (CPR) and cytochrome b_5 (b5) at physiologically relevant concentrations. Finally, all the drug-metabolizing enzymes that are present in HLMs are in physiologically relevant ratios, which is important in that *in vitro* data suggest that protein–protein interactions may occur that can alter enzymatic activity, and are dependent on ratios of the enzymes involved. To use HLMs, one simply adds a physiological pH (7.4) maintaining buffer, the enzyme cofactor nicotinamide adenine dinucleotide phosphate (NADPH), and substrate [3,4]. Since multiple enzyme isoforms are present in the preparation, determining the individual isoform(s) involved may be somewhat less straightforward but can be accomplished by coincubation with isoform-specific inhibitors or antibodies [5].

As with any system, there are also disadvantages to the use of HLMs for determining enzyme activity and isoform involvement. Depending on the time between tissue harvest, microsome preparation, and freezing, enzyme activity can be lost to varying degrees depending on the time duration. Freezing whole liver tissue first, then thawing and preparing HLMs can also reduce enzyme activity. In addition, once thawed for use, HLM preparations usually only maintain consistent activity levels for up to 1 h at 37°C, the usual temperature for conducting *in vitro* HLM incubations. It should also be realized that HLMs will not contain either cytosolic enzymes (e.g., SULTs) or transporter proteins [e.g., P-glycoprotein (PgP)]. This lack of the total complement of enzymes precludes evaluation of "total" metabolism of a compound if multiple enzyme families are involved. However, since both UGT and P450 enzymes are present in HLMs, one can add the necessary cofactors for both to permit simultaneous activity by both enzyme systems and thus, to evaluate the overall metabolism by both systems, though this requires care in determining the incubation conditions. More typically, each route of metabolism is evaluated separately. Finally, it should be realized that HLM preps do not contain the necessary machinery for enzyme synthesis and thus, cannot be used for enzyme induction experiments. In spite of these limitations, HLMs remain the primary "workhorse" of drug metabolism studies, given their relatively low cost, ease of use, and availability.

While study on CYPs in HLMs essentially only requires NADPH as a cofactor and an appropriate buffer, the study on UGTs require more involved conditions. Like with the CYPs, a cofactor, uridine-5′-diphosphoglucuronic acid (UDPGA), that provides the glucuronic acid for transfer also needs to be included [6]. However, in contrast to the CYPs, since UGT proteins exist with their active side facing the luminal part of the endoplasmic reticulum, access to substrates and cofactors requires them to pass

through the membrane to access the active enzyme site. Hence, membrane disruptors such as alamethicin (pore-forming agent), sonication, or use of a surfactant (e.g., Brij 58) are required to obtain activities that are readily measurable. Disruption of the membrane is usually conducted on ice for a period of 15–30 min before beginning incubation with substrate. Saccharolactone, a β-glucuronidase inhibitor is sometimes also added to prevent an artificial lowering of UGT activity [7]. Finally, recent research has suggested that a number of K_m values generated earlier may have been artificially elevated due to the presence of inhibitory long-chain unsaturated fatty acids in the incubations that can compete with substrates for the UGT active site. However, it appears that the inclusion of albumin can restore K_m to values that result in more accurate IVIVC predictions. Thus, some researchers advocate for the inclusion of albumin in all incubations evaluating UGTs; however, this opinion is not shared by all.

FMOs are a microsomal enzyme that can metabolize soft nucleophiles, such as nitrogen- and sulfur-containing compounds and, in particular, heterocycles with these atoms. Since FMOs can catalyze analogous reactions to the CYPs, such as N- and S-oxidation, it is important to distinguish between the two enzyme families to assure the correct implications are made. The incubation conditions for FMOs are the same as CYPs, that is, it requires substrate, NADPH, and buffer but at a slightly alkaline pH of 8–9 for optimal activity. To distinguish between CYP and FMO metabolism, the microsomal mixture can be incubated at 45°C for 5 min in the absence of NADPH, causing degradation of the FMOs but leaving the CYPs unaffected. The reaction is then carried out under normal conditions and if the activity goes away, the implication is that FMOs were involved since they would have been degraded during the preincubation. Nonionic detergents that inhibit CYPs but not FMOs can also be used to delineate between the two enzyme families.

9.3.2 Expressed Enzymes

With current technology, almost any individual P450 isoform human or animal cDNA can be expressed in cell systems, such as *Escherichia coli* bacteria, yeast, or insect cells (e.g., *Trichoplusiani*), and the resulting enzymes can subsequently either be fully purified or membrane preps can be generated [8,9]. In addition, CPR or b5 can be coexpressed in these cells (with membrane preps as the final form) [10,11]. The enzymes thus obtained are suitable to determine kinetics of a substrate from a single P450, assuming that the cDNA from only a single enzyme was expressed. Expressed enzymes are the simplest system and can provide unequivocal evidence of the ability (or lack of ability) of an enzyme to metabolize a substrate. Expressed enzymes also allow for discernment of the reaction kinetics of a single enzyme, which may be confounded by multiple enzyme involvement in systems with the full enzyme complement. Expressed enzymes offer additional advantages that make them an attractive system in certain circumstances. For example, because only one enzyme is present, they can used to identify isoforms that make a minor contribution to the metabolism of a substrate that might become more important when the primary isoform is inhibited [12]. This situation would be difficult to discern in a system with the full complement of enzymes that might overshadow this contribution by a more minor enzyme. Hence, expressed enzymes can provide comprehensive information on all the isoforms metabolizing a substrate. In addition, atypical kinetics (see below) are also most accurately elucidated using single enzyme systems, since confounding may occur in multiple enzyme systems

[3]. Finally, expressed systems allow the most convenient study of the kinetics of polymorphic enzymes, since allelic variants are easily expressed in sufficient quantities in these systems. Locating and genotyping sufficient quantities of, for example, HLMs, expressing an allelic variant, is currently difficult.

Incubations using expressed enzymes are, as with microsomes, a straightforward affair with only the addition of an appropriate cofactor [such as NADPH for P450s, 3′-phosphoadenosine-5′-phosphosulfate (PAPS) for the SULTs, and UDPGA for UGTs], buffer at pH 7.4 and the substrate being required. These systems are generally robust enough to provide activity for up to 45 min with a subsequent drop in activity and also hardy enough to withstand a few freeze thaw cycles. Expressed enzyme preparations of CYPs, UGTs, *N*-acetyltransferases (NATs), FMOs, aldehyde oxidases (AOs), SULTs, monoamine oxidases, and esterases are now commercially available and are valuable tools in reaction phenotyping and metabolic pathway elucidation.

It should be realized that expressed enzymes also possess certain disadvantages. For example, since they do not contain the full complement of enzymes, overall clearance is more difficult to estimate and the relative importance of individual enzymes may be overestimated. The fact that a substrate is metabolized by an enzyme in a single-enzyme system does not indicate that this will be observed *in vivo* since a number of variables such as enzyme ratios, ratios of redox transfer proteins (see below), and unbound substrate concentrations at the enzyme active site can influence the metabolism. Also, the concentrations of CPR and b5 used in the expressed enzyme systems are designed for maximal activity and are not reflective of physiological levels. In addition, for fully purified enzymes, lipid vesicles (typically prepared from dilauroylphosphatidylcholine or didecanoylphosphatidylcholine) need to be added to the system as an artificial membrane system to provide a milieu for the hydrophobic portions of the enzyme to anchor. This again is an artificial system and may not be fully representative of complex *in vivo* architecture and interactions. These kinds of systems are termed *reconstituted expressed enzymes*, as opposed to expressed systems, wherein the enzyme is maintained in the membrane environment of the cell system.

A reconstituted recombinant enzyme incubation requires the expressed CYP enzyme, lipid vesicles, appropriate level of CPR (2:1 or greater CPR:P450), b5 (1:1 or greater b5:P450), reaction buffer at pH 7.4, and NADPH, all maintained at 37°C. Since this incubation typically requires a greater number of constituents to be mixed as compared with HLMs, there is typically greater variability in kinetic parameters depending on ratios, order of addition, type of lipids used, and so on. In addition, some P450s such as CYP3A4 are more challenging to reconstitute into lipids and elicit activity, as opposed to others such as CYP2C9 and CYP2D6. Clearance predictions can be made from expressed enzymes, but this usually requires incorporation of a relative activity factor (RAF) established using probe substrates of the enzyme to standardize the activity of the P450 isoform to microsomal activity and an accounting for the relative ratios of each enzyme in a typical liver system [13].

Recently, the issue of CYP enzyme protein–protein interactions has been discussed [14,15] adding an additional layer of potential complexity. In these cases, the presence of a second CYP isoform can modulate (either increase or decrease) the activity of the second isoform. Since expressed enzyme systems typically involve the incubation of a single CYP isoform, one would not expect these interactions to occur in this type of system. However, if these do occur in HLMs, conjectured but not conclusively

proven, then the *in vitro–in vivo* extrapolations made from expressed enzyme systems involving a single isoforms may be less accurate than anticipated. A second potential complication can occur when expressed enzymes are mixed in a cocktail fashion for studying enzyme involvement and inhibition interactions, since these protein–protein interactions may then occur in these expressed enzyme incubations containing more than one CYP isoform.

9.3.3 Human Hepatocytes (Fresh and Cryopreserved)

Human heptocytes contain the entire complement of drug-metabolizing enzymes, induction machinery, and most transporters [16,17]. They also contain all the cofactors and other redox proteins in appropriate levels [18]. Thus, they provide a system very similar to an actual human liver (with the exceptions of blood flow and intercellular interactions). They can be used for longer (e.g., 8–10 h) experiments and hence, may be more beneficial in the study of slowly cleared substrates, though it should be realized that the activity of hepatocytes does decline with time [19,20]. A significant advantage of human hepatocytes (either fresh or cryopreserved) is their ability to synthesize new enzyme protein and thus, they are ideally suited for enzyme induction experiments. The second primary advantage of human hepatocytes is that they contain the full complement of enzymes and transporters and thus, are ideally suited to evaluate total clearance by metabolism and transport. However, this may also be a disadvantage if one wishes to identify the specific isoform(s) involved in metabolism or the kinetics of an individual process.

Fresh hepatocytes, isolated from donor livers, can be maintained in appropriate media and be utilized to determine enzyme kinetics. However, fresh hepatocytes are less readily available, more difficult to maintain than, for example, HLMs. They are also expensive and need to be used relatively soon after donor harvest and preparation [21,22]. Because this timeframe from harvest to preparation and final use can be variable in length, it is not uncommon to observe substantial intersubject variability. Additionally, it should be realized that since hepatocytes are obtained from recently deceased donors, liver function may have been compromised and multiple drugs may have been present at harvest. This could lead to induction or inhibition of the metabolizing enzymes. The extensive handling procedures and expensive materials cost offset some of the advantages of using fresh hepatocytes. Cryopreserved hepatocytes were developed to overcome some of the disadvantages of freshly isolated hepatocytes. These hepatocytes are cryogenically frozen and thus, can be stored for long periods before use, making them more attractive than fresh hepatocytes that typically need to be used within a few days of extraction [23,24]. Cryopreserved hepatocytes can also be pooled, as is done with microsomes, to reduce the impact of interindividual variation. Though originally less active, recent advances in preparation and preservation techniques have resulted in cryopreserved hepatocyte preparations with activity similar to freshly isolated hepatocytes [23].

Incubations with cryopreserved hepatocytes have been standardized by suppliers of these tissues. Thawing and reconstitution of these cells, followed by incubation with buffer and substrate is the typical protocol. Fresh hepatocytes do not require the thawing and reconstitution steps that are required of cryopreserved hepatocytes, but may require additional Percoll filtration steps to improve viability. Since hepatocytes

contain all the necessary cofactors and additional proteins, no additional components need to be added to the media, although these incubations are typically done in 5% CO_2 at 37°C. Recent reports also suggest that cryopreserved hepatocytes, due to the process of instant freezing, are better suited for the study of AO activities that tend to be lost in fresh hepatocytes within 24 h post isolation [25].

9.3.4 Liver Slices

Liver slices are prepared from liver tissue using a microtome to create ultrathin slices. They contain all the drug-metabolizing enzymes and transporters, allow for intercellular communication, and in addition the role of passive diffusion can be elucidated [26,27]. However, liver slices exhibit a rapid decrease in activity (and typically activity lower than hepatocytes), are subject to interslice variation, cannot be pooled to overcome interindividual variation, are expensive to produce, and require special equipment to produce [28]. For these reasons, liver slices are not frequently used in kinetics determination.

9.3.5 S9 Fraction

The S9 fraction, such as microsomes, is prepared by homogenization of the tissue followed by ultracentifugation to isolate the desired fraction. In this case, the S9 fraction is the supernate typically resulting from the spin before the $100,000g$ spin that is used to isolate the microsomes. Thus, this fraction of tissue will also contain the cytosolic and mitochondrial enzymes, though the activity can be lower than that of the microsomal fraction [29]. The presence of cytosolic conjugative enzymes such as SULTs, NATs, AO, and xanthine oxidases make the S9 fraction a more versatile system than microsomes. Though at one time used to measure overall metabolism, the requirement to add necessary cofactors and the availability of human hepatocytes has reduced the use of S9 fractions in determining enzyme kinetics and drug metabolism reactions. Incubation conditions for S9 fractions are similar to those with microsomes, that is, substrate, buffer, and appropriate cofactor need to be added. Typically, higher concentrations of protein, 2–4 mg/mL final, are used due to the inherent diluted nature of this system.

AOs are being increasingly recognized for their role in drug disposition, are a cytosolic enzyme, and hence found in S9 and cytosolic fractions and hepatocytes [30]. Their use does not require any special incubation conditions apart from enzyme, substrate, buffer, and recognition. Esterases are present ubiquitously, and hence, any tissue fraction, be it microsomes, cytosol, or a tissue homogenate, can be used to determine the esterase activity and substrate specificity. No unique cofactors are required to be added for esterase activity.

In contrast to the above cytosolic enzymes, the SULTs, another cytosolic drug-metabolizing enzyme, require addition of the cofactor PAPS to supply the sulfate group that is transferred onto the phenolic oxygen during an SN_2 substitution reaction. Similarly, NATs can be assayed for activity in cytosolic protein or S9 at protein concentrations of 0.2–1 mg/mL, 1 mM ethylenediaminetetraacetic acid (EDTA), dithiothreitol (1 mM; optional), phosphate buffer, pH 7.4, and acetyl CoA (2 mM). Acetyl CoA is the cofactor supplying the acetyl group that is added onto a nitrogen atom.

9.3.6 HepaRG Cells

The HepaRG cell line was created following immortalization of liver cells from a donor with hepatocellular carcinoma [31]. The cells were subsequently cultured and passaged with the cells then differentiated by the addition of dimethyl sulfoxide (DMSO). Once DMSO is added to the medium, the cells differentiate into hepatocyte-like granular cells with one or two nuclei. In addition, during this process, bile cannicular-like structures are formed [32]. As compared with isolated human hepatocytes, HepaRG cells exhibit comparable or greater levels of many drug-metabolizing enzymes (CYP1A2, CYP2B6, CYP2C9, CYP2E1, and CYP3A4, SULTs, UGTs, and glutathione-*S*-transferases), transporters, and induction elements (constitutive androstane receptor, peroxisome proliferator-activated receptors, aryl hydrocarbon receptor, and pregnane X receptor) [33,34]. In addition, the bile cannicular-like structures provide another level of detail and physiology to these cells [35,36]. Endogenous proteins such as albumin, haptoglobin, and aldolase B are also present in these cells [34]. Together, these factors suggest that HepaRG cells are very similar in morphology and physiology to liver cells, making them an appropriate system to study enzyme kinetics, inhibition, induction, and long-term toxicity. In addition, the HepaRG cells are stable for up to two weeks after differentiation and hence are useful to study slowly metabolized substrates, as well as conduct long-term toxicity and mutagenicity studies.

However, there are some identified disadvantages of HepaRG cell lines. For example, at the present time, they do not contain all P450s at physiologically appropriate ratios—for example, CYP2D6 is not present since the donor may have been a CYP2D6 poor metabolizer [34]. In addition, since it is a cell culture system, constant maintenance is required and sufficient time must be allowed (over 30 days) for the cell line to be cultured and differentiated. Despite these disadvantages, the HepaRG cell line appears to have promise toward providing qualitative and quantitative information on drug metabolism, although further characterization of activity and enzyme levels is required.

9.4 BASICS OF ENZYME KINETICS

9.4.1 Michaelis–Menten Kinetics

Enzyme kinetics are assumed to be governed by processes that are saturable and can be described mathematically by the Michaelis–Menten (Michaelis–Menten, sometimes called *Henri–Michaelis–Menten equation*) equation (Eq. 9.1), which states that at low concentrations of substrate, a first-order linear relationship exists between the rate and substrate concentration, and at high saturating concentrations of substrate, the rate is independent of substrate concentration and reaches a maximal value [37]. This maximal value is termed V_{max} or the maximum velocity, while half the concentration required to achieve this maximum velocity is termed K_m. With respect to the single-substrate reaction (Scheme 9.1), it should be realized that K_m is equal to $(k_{-1} + k_2)/k_1$ and thus is the amalgamation of several rate constants. With respect to affinity, unfortunately, K_m is frequently (and incorrectly) used interchangeably with $K_S (K_S = k_{-1}/k_1)$, which is the substrate dissociation constant. Though K_m may sometimes approximate K_S when k_2 is very small relative to k_1 and k_{-1}, the two do not have to be equal, and numerous examples exist where these parameter values vary dramatically. V_{max} is

$$E + S \underset{k_{-1}}{\overset{k_1}{\rightleftharpoons}} ES \xrightarrow{k_2} E + P$$

Scheme 9.1

indicative of the capacity of the enzyme to turnover that particular substrate, a higher V_{max} indicates faster turnover of substrate. The kinetic scheme and equation governing Michaelis–Menten equation are given as follows:

$$v = \frac{V_{max} \cdot [S]}{K_m + [S]} \tag{9.1}$$

where $V_{max} = k_2 \cdot [ES]$, which is a measure of the rate of product formation, $K_m = (k_{-1} + k_2)/k_1$ is the Michaelis constant, and $K_S = k_{-1}/k_1$ is the dissociation constant for the ES complex.

Figure 9.1a depicts the classic hyperbolic enzyme kinetics plot. Several assumptions have been made in the generation of the Michaelis–Menten equation. It is assumed that the [ES] complex is in a quasi-steady state, that is, its rate of concentration change

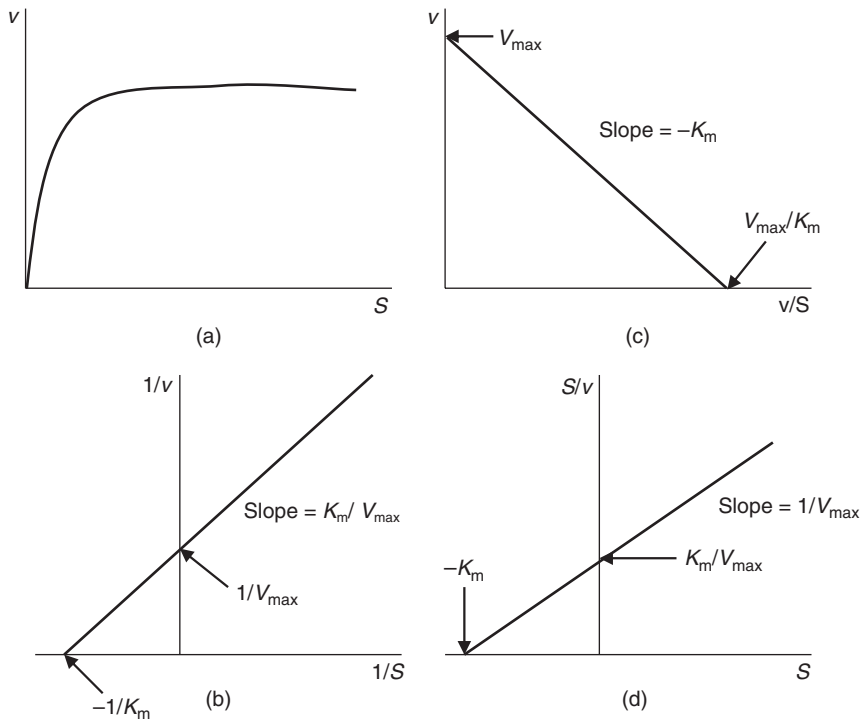

Figure 9.1 Kinetics of enzymes following Michealis–Menten (MM) kinetics: (a) the classic hyperbolic plot, (b) the Lineweaver–Burk (LB) double reciprocal plot, (c) the Eadie–Hofstee (EH) plot, and (d) the Hanes–Woolf plot. EH, LB, and EH plots can be used for determining whether the data follows MM kinetics, while all plots can be used for determination of the kinetic parameters—V_{max} and K_m.

is zero since each molecule of [ES] converted to product is replenished instantly. The other key assumption is that total enzyme concentration is constant and is the sum of free enzyme, [E], and the [ES] complex. Additionally, the concentration of the substrate is much higher than the enzyme, and this combined with the total enzyme concentration being constant implies that the rate has a pseudo-first-order dependence on substrate concentrations (at low nonsaturating substrate concentrations).

The Michaelis–Menten equation can be rewritten into a number of forms to allow for easier visual analysis of the data and calculation of kinetic parameters [37] (Fig. 9.1).

9.4.2 Lineweaver–Burk (LWB) Double Reciprocal Plot

$$\frac{1}{v} = \frac{K_m}{V_{max}} \cdot \frac{1}{[S]} + \frac{1}{V_{max}} \tag{9.2}$$

The Lineweaver–Burk (LWB) plot depicts the reciprocal of velocity versus substrate concentration and results in a straight line with a slope equal to K_m/V_{max}, a y-intercept representative of $1/V_{max}$, and an x-intercept equal to $-1/K_m$ (Fig. 9.1b).

9.4.3 Eadie–Hofstee (EadieHofstee) Plot

$$v = -K_m \cdot \frac{v}{[S]} + V_{max} \tag{9.3}$$

The Eadie–Hofstee (EadieHofstee) plot is graphically represented as v versus $v/[S]$ and results in a straight line with slope equal to $-K_m$, with the y-intercept representing V_{max} and the x-intercept equal to V_{max}/K_m (Fig. 9.1c).

9.4.4 Hanes–Woolf Plot

$$\frac{[S]}{v} = \frac{1}{V_{max}}[S] + \frac{K_m}{V_{max}} \tag{9.4}$$

In the Hanes–Woolf plot, where it is plotted as $[S]/v$ versus [S], giving a straight line with a slope representative of $1/V_{max}$, where the y-intercept is equal to K_m/V_{max} and the x-intercept is equal to $-K_m$ (Fig. 9.1d).

Though each of the above graphical representations can give quick estimations of the kinetic parameters K_m and V_{max}, in general, nonlinear regression fitting of the data to the Michaelis–Menten model is preferred for more accurate estimations. These types of nonlinear regression fits have been made easier with the advent of inexpensive, readily available, and easy to use kinetic modeling programs.

The first step in determination of enzyme kinetics, viz V_{max} and K_m values, or depletion rate constants, is the verification of time and protein (enzyme concentration) linearity. One must assure that the proposed length of the incubations is not so long that metabolite formation rates are affected by enzyme degradation and that the conditions do not consume all cofactors, such as NADPH or too much substrate that could also affect metabolite formation rates. To accomplish assurance of linearity of time, one usually conducts incubations at 4–5 time points, typically ranging from 5

to 45 min. In the case of enzyme concentration, again, 4–5 protein concentrations are employed. With regard to substrate concentration, a concentration near the expected V_{max} or at least equal to the expected K_m should be employed. Finally, determination of enzyme kinetics is also based on the assumptions of rapid equilibrium and steady-state conditions. To this end, the investigator should assure that <10% substrate consumption occurs throughout the experiment to maintain steady-state conditions. Obviously, the above methodologies are dependent on the ability to measure the formation of metabolite, as the measurement of the amount of "product" formed.

9.4.5 Use of Substrate Depletion Methods to Determine Enzyme Kinetics

Early in the drug discovery process, it is desirable to obtain estimates of clearance rates for the molecule to assess its viability for further development, before metabolic pathways of drug removal have been determined, and before expending significant resources and time to synthesize metabolite(s). While the traditional methods of assuring time and protein linearity as well as steady-state kinetics for the determination of enzyme kinetics is preferred, many less labor-intensive methods also exist. Since K_m values are in general of greater interest in the drug development process than V_{max} values, determining K_m from a substrate disappearance $t_{1/2}$ assay has been described and the theoretical validation of the technique explained [38,39]. The first-order rate of degradation of substrate over a range of substrate concentrations is determined, and the inflection point of the plot of first-order rate versus substrate concentration can give a very reasonable approximation of K_m. It should be noted that determination of the substrate disappearance $t_{1/2}$ for the prediction of *in vivo* clearances should typically be done at substrate concentrations well below K_m to assure linearity. However, K_m values are generally not known for new chemical entities, and hence, in an attempt to assure substrate concentrations below K_m, typically $1\,\mu M$ substrate concentration is utilized.

P450 kinetics has been extensively studied and K_m values from submicromolar to millimolar range have been obtained. Compounds with submicromolar K_m values typically are good substrates and can sometimes display saturable metabolism *in vivo*. The observed range of K_m values for UGTs has been reviewed extensively by Kiang *et al*. [40]. While UGTs are in general considered to be high K_m reactions, a closer analysis reveals that a wide range of K_m values starting from single digit micromolar ($5\,\mu M$) up to millimolar levels have been observed. However, the bulk of K_m values observed for the UGTs are in the double digit micromolar range and above, suggesting that saturation kinetics will not be observed *in vivo* since drug concentrations seldom reach this range. Even with K_m values in the range of $5\,\mu M$, the risk of nonlinear kinetics (due to saturation of clearance) for the UGTs is less likely when only unbound concentrations of the drug is considered.

In the case of the FMOs, the reported K_m values are in a much tighter range, from around $2.5\,\mu M$ to approximately $60\,\mu M$ [41–49]. For AOs, a molydboflavoprotein that prefers to oxidize carbons with low electron density (nitrogenous heterocyles) [50,51], the reported K_m values have ranged from $3.4\,\mu M$ to upward of $400\,\mu M$ [52–55]. As suggested from these reports, K_m values for the FMOs and AOs are rarely in the low single digit micromolar concentrations, and hence, a $1\,\mu M$ starting substrate concentration for $t_{1/2}$ determinations is appropriate for these enzymes. However, for

the sulfonyltransferases, the K_m values span a broader range (0.5 μM to $\sim$1 mM) [56–63], but generally are in the low micromolar range.

One should use the lowest possible protein concentration to minimize nonspecific protein binding and to be cognizant of incubation time as microsomes are generally stable for only 45–60 min [64]. Also, it should be realized that a minimum of 15–20% of the drug needs to be cleared to provide sufficient analytical resolution. In the case of slowly cleared substrates, large errors may be introduced due to difficulty in dissecting the rate of depletion of substrate from analytical error. Substrate depletion methods can be used to determine half-lives that are used in estimating intrinsic clearances [65] (see Section 9.6).

9.4.6 Caveats to be Considered in the Determination of Enzyme Kinetics

The effects of solvents on the activity of enzymes also require special consideration, since most drug candidates are nonpolar and require some solvent component for dissolution. Numerous studies have demonstrated that various organic solvents can either activate or inhibit different isoforms, depending on the substrate and enzyme source. For example, at concentration of 0.3%, methanol and acetonitrile had no effect on CYP1A1, CYP2D6, CYP2B6, and CYP2C9. However, at a concentration of 1%, methanol inhibited these same enzymes by 12–26% and acetonitrile inhibited CYP1A1, CYP2B6, CYP2A6, CYP3A4, CYP2C19, and CYP2D6 by 10–60%, depending on the isoform. In contrast, even at concentrations as low as 0.1%, DMSO inhibited CYP3A4, CYP2C19, and CYP2D6 by 15–25% [66]. Ideally, one should try to use $<$0.3% of methanol or acetonitrile to dissolve substrates, though when not feasible, one should use as little organic solvent and preferably $<$1%.

9.5 ATYPICAL ENZYME KINETICS

While Michaelis–Menten kinetics are the most commonly observed kinetics among the drug-metabolizing enzymes, there is a growing database of substrate–enzyme combinations that display atypical kinetics. These non-Michaelis–Menten kinetics have been observed most frequently in CYP3A4 and CYP2C9, and they have also been observed in CYP2D6, CYP1A2, and CYP1A1. In addition to P450s, SULTs, UGTs, and PgP, transporter proteins have also been observed to demonstrate atypical kinetics. The application of the Michaelis–Menten equation to substrate metabolism displaying atypical kinetic behavior may result in errors in the estimation of *in vitro* intrinsic clearance, which is subsequently used in the estimation of *in vivo* clearance. Atypical kinetics is generally believed to occur when two substrate molecules (either two molecules of the same substrate or two different substrates) are present in the active site simultaneously [67]. It should, however, be recognized that multiple conformers of the enzyme or enzyme dimers [68] have also been suggested to contribute to the occurrence of atypical kinetics.

The following sections describe the various kinds of atypical kinetics, the equations governing them, and the diagnostic plots to determine the nature of the kinetics [69–72]. While this chapter focuses predominantly on CYPs, it should be noted that SULTs, UGTs, and transporters also display atypical kinetics. These have been reviewed previously and hence are not dealt with here [73].

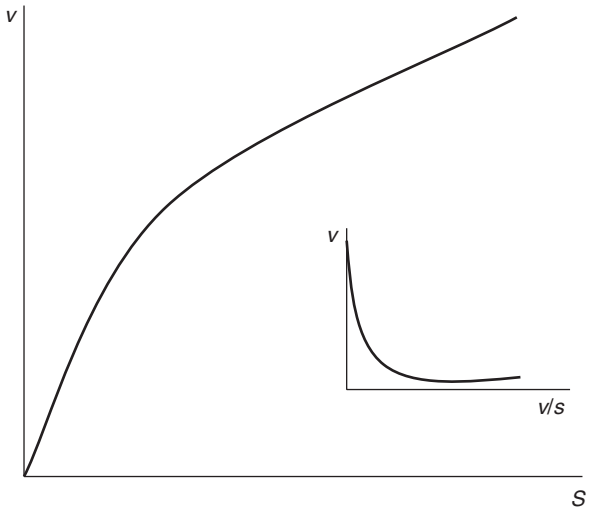

Figure 9.2 Biphasic kinetics. The inset shows the diagnostic EH plot for the same.

9.5.1 Biphasic Kinetics

Biphasic kinetics (Fig. 9.2) is observed when the metabolite formation rate appears to initially behave as if it would begin to saturate but instead continues to increase in a linear fashion, such as that occurring with the CYP2C9 substrate naproxen [67]. In this case, two molecules of the same substrate are present in the enzyme active site. One of the catalytic sites behaves as a low K_m and low V_{max} (high "affinity," low capacity) site, while the other catalytic site behaves as a high K_m and a high V_{max} site (low "affinity," high capacity). Hence, at low substrate concentrations, the first catalytic site is more represented in the velocity–substrate plot, while at higher substrate concentrations closer to K_{m2}, the second catalytic site is more prominent. As seen in Fig. 9.2, saturation is not observed, but a linear increase in velocity is observed at high substrate concentrations. The EadieHofstee plot for this kind of kinetics is shown in Fig. 9.2 (inset). This type of plot will also be visible if two enzymes are present and both catalyze a single-substrate reaction, one enzyme with a low V_{max} and K_m and the other enzyme with a high V_{max} and K_m. When a substrate exhibits biphasic kinetics, but the Michaelis–Menten equation is incorrectly applied, an underprediction of clearance (V_{max}/K_m) typically occurs. When substrate depletion experiments are used to determine intrinsic clearance, one must be careful to use an appropriate substrate concentration (typically as low as possible, e.g., $1\,\mu M$ or lower) so as to best reflect metabolism at the low K_m site (which is typically nearer actual physiological concentrations of the drug), rather than a higher concentration that might reflect the high K_m site and typically not physiological.

The equation used to describe biphasic kinetics (Eq. 9.5) is as follows:

$$v = \frac{(V_{max\,1} \cdot [S]) + Cl_{int}{}^{*}[S]^2}{K_{m1} + [S]} \tag{9.5}$$

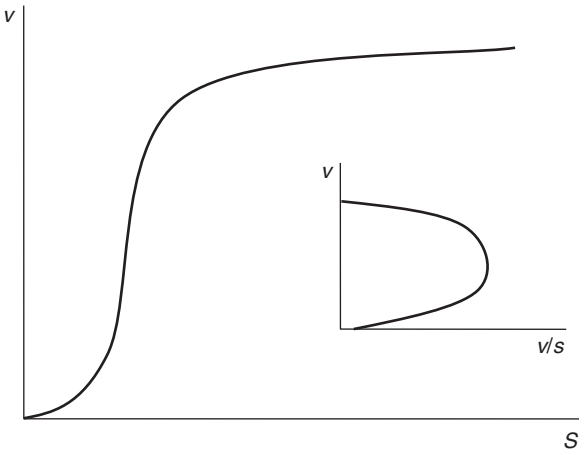

Figure 9.3 Autoactivation kinetics. The inset shows the diagnostic EH plot for the same.

where $V_{max\,1}$ and K_{m1} are the parameters governing the first catalytic site and Cl_{int2} is (V_{max2}/K_{m2}) for the second catalytic site, that is, Cl_{int2} is the slope of the linear portion of the plot that occurs at high substrate concentrations.

9.5.2 Autoactivation (Sigmoidal Kinetics)

Autoactivation (Fig. 9.3) occurs when a substrate activates its own metabolism, again presumably when two substrate molecules occupy the active site at the same time resulting in a sigmoidal kinetic profile [67]. Detecting sigmoidal kinetics can be challenging since the changes in the substrate–velocity plot at low substrate concentrations are often subtle, sometimes making it difficult visually to distinguish from Michaelis–Menten kinetics. Thus, it is suggested that the data be plotted in an EadieHofstee plot (Fig. 9.3, inset) to better assess the type of kinetics being exhibited. It should be recognized that sufficient analytical sensitivity and precision are also paramount in establishing autoactivation kinetics. When autoactivation (sigmoidal) kinetics are observed in a two binding site model, $V_{max\,2} > V_{max\,1}$ (when $K_{m1} = K_{m2}$) or $V_{max\,1} = V_{max\,2}$ (when $K_{m2} < K_{m1}$) [67]. Hence, two independent solutions exist to the sigmoidal equation. The two binding sites can have naturally differing V_{max} and K_m values, or the binding of the first substrate molecule could cause a conformation change in the enzyme active site, thereby altering the V_{max} and K_m values of the second binding site. If the V_{max} and K_m values of the two binding sites are similar in values, then a hyperbolic profile will be visible. Use of the Michaelis–Menten equation to predict kinetic parameters for a substrate exhibiting autoactivation kinetics will result in an estimation of V_{max} and K_m more reflective of the high V_{max} site, most likely leading to an underestimation of intrinsic clearance at the more physiologically relevant concentrations that usually occur near K_m of the lower V_{max} site. In substrate depletion experiments, as with biphasic kinetics, the starting substrate concentration will determine whether the intrinsic clearance of the first or second catalytic site is estimated.

The Hill equation (given below) can be used for a simplistic fit of autoactivation data:

$$v = \frac{V_{\max} \cdot [\mathrm{S}]^n}{K' + [\mathrm{S}]^n} \tag{9.6}$$

where n is the degree of cooperativity; a value of n equal to unity represents no autoactivation, whereas a value of $n > 1$ suggests cooperativity and thus, sigmoidicity. Note that this equation gives the parameter K', which is analogous to, but not the same as, K_{m}. If a sufficient number of data points are employed, one can use Equation 9.7 to estimate the $V_{\max}$ and K_{m} values for each of the two binding sites:

$$v = \frac{\dfrac{(V_{\max 1} \cdot [\mathrm{S}])}{K_{\mathrm{m1}}} + \dfrac{V_{\max 2} \cdot [\mathrm{S}]^2}{K_{\mathrm{m1}} \cdot K_{\mathrm{m2}}}}{1 + \dfrac{[\mathrm{S}]}{K_{\mathrm{m1}}} + \dfrac{[\mathrm{S}]^2}{K_{\mathrm{m1}} \cdot K_{\mathrm{m2}}}} \tag{9.7}$$

where $V_{\max 1}$ and K_{m1} are the kinetic parameters for the first binding site and $V_{\max 2}$ and K_{m2} for the second binding site.

9.5.3 Heteroactivation

Heteroactivation occurs when coincubation with another molecule (effector) results in an increase in the metabolism of the primary substrate [67,74]. The effector molecule is frequently also a substrate for the same enzyme, but this is not an absolute requirement. Importantly, in the case of heteroactivation coincubation of substrate, the effector does not result in inhibition of the primary substrate, as might be expected. It is generally believed that as with the other atypical kinetics phenomena discussed herein, the effector and substrate are believed to be present in the active site simultaneously, despite the fact that they are different molecules. It should also be noted that effector molecules binding to an allosteric site outside the active site have been reported [75], possibly causing conformational changes within the active site that might result in cooperativity. It has also been observed that the effector molecule is capable of undergoing metabolism simultaneously with the substrate [10]. This suggests that both the effector and substrate are present simultaneously in the catalytic region of the enzyme [67,76]. The following equation has been used to describe data exhibiting heteroactivation kinetics:

$$v = \frac{V_{\max} \cdot [\mathrm{S}]}{K_{\mathrm{m}} \dfrac{\left(1 + \dfrac{[\mathrm{B}]}{K_{\mathrm{B}}}\right)}{\left(1 + \dfrac{\beta[\mathrm{B}]}{\alpha K_{\mathrm{B}}}\right)} + [\mathrm{S}] \dfrac{\left(1 + \dfrac{[\mathrm{B}]}{\alpha K_{\mathrm{B}}}\right)}{\left(1 + \dfrac{\beta[\mathrm{B}]}{\alpha K_{\mathrm{B}}}\right)}} \tag{9.8}$$

where the parameter α is related to the change in K_{m} due to the presence of the effector ($\alpha < 1$ is reflective of a decrease in K_{m}), β represents change in $V_{\max}$ due to the presence of the effector ($\beta > 1$ is reflective of an increase in $V_{\max}$), [B] is the effector concentration, and K_{B} is the dissociation constant of the effector.

Obviously, when determining the clearance of substrates *in vivo*, one does not include a second substrate molecule and so though V_{max} and K_m are affected by heteroactivation, it would not be operable in typical enzyme kinetics incubations. However, during *in vitro* drug–drug interaction exploration, heteroactivation can be problematic as it will be difficult to predict the degree of interaction that will occur *in vivo*. Studies have been conducted to determine whether heteroactivation occurs *in vivo*. *In vitro* studies demonstrated that diclofenac metabolism by CYP3A4 is stimulated in the presence of quinidine [77]. To assess whether this phenomenon also occurs *in vivo*, the metabolism of diclofenac in monkeys in the presence and absence of quinidine was studied and it was observed that an ~57% decrease in the plasma concentration of diclofenac was observed when quinidine was coadministered as compared with diclofenac alone [78]. In humans, demonstration of heteroactivation has been less clear. Hutzler *et al*. [79] were only able to demonstrate an ~10% activation of flurbiprofen metabolism by dapsone in humans, despite substantial heteroactivation occurring *in vitro*. Though not directly studied, Egnell *et al*. [80], using a meta-analysis from multiple studies, predicted based on modeling that the coadministration of felbamate resulted in a 20–47% increase in the ratio of carbamazepine-epoxide to carabamazepine plasma concentrations due to heteroactivation of CYP3A4-mediated carbamazepine metabolism. A recent study examined the heteroactivation of CYP3A4-mediated metabolism of the dye Nile Red with α-naphthoflavone as an activator [81]. α-Naphthoflavone affected the sequential kinetics of Nile Red and increased the catalytic efficiency of the secondary metabolite production at the expense of the primary metabolite. Another recent paper provides the closest biophysical evidence for a two-site model based on longitudinal T_1 NMR relaxation and docking studies on carbamazepine-mediated heteroactivation of midazolam metabolism by CYP3A4. Midazolam metabolism typically results in greater quantities of 1′-OH-midazolam compared with 4-OH-midazolam when incubated with CYP3A4. However, this ratio declines in the face of high midazolam concentrations or the presence of carbamazepine. The distances of protons at the site of metabolism as determined from the NMR studies were used in docking simulations to demonstrate that when a single molecule of midazolam is present in the active site of CYP3A4, the 1′-CH_3 position of the molecule is closer to the catalytic heme, hence leading to the production of more 1′-OH-midazolam as compared with 4-OH-midazolam. However, at higher midazolam concentrations and when midazolam and carbamazepine are coincubated, two midazolam molecules or one midazolam molecule and one carbamazepine molecule assume a stacked position within the active site. This is predicted to result in the 4′-position of midazolam being oriented closer to the active heme than the 1′-CH_3 position. This observation could explain the shift in ratios of 1′-OH-midazolam to 4-OH-midazolam on homo- or heteroactivation.

9.5.4 Substrate Inhibition

Substrate inhibition (Fig. 9.4) occurs when, at high concentrations of the substrate, the velocity of metabolite formation decreases [67]. Figure 9.4 (inset) depicts the EadieHofstee plot for substrate inhibition. Substrate inhibition is also thought to occur due to the presence of two molecules of the same substrate in the active site simultaneously. In the case of non-overlapping binding sites, substrate inhibition is observed when $V_{max\,2} < V_{max\,1}$ (and $K_{m1} = K_{m2}$ or $K_{m1} > K_{m2}$). When K_m and V_{max} of both sites are similar, substrate inhibition can still occur if a substrate molecule binding to

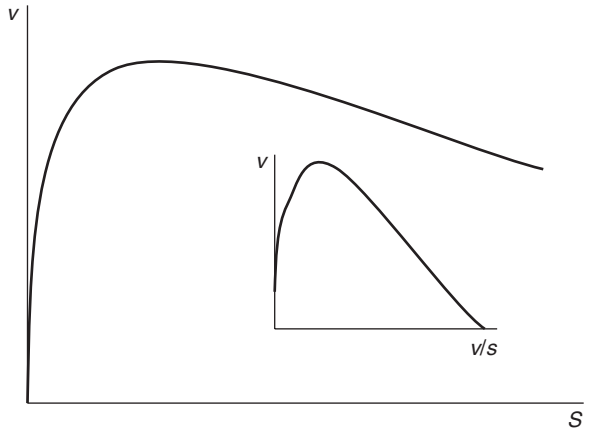

Figure 9.4 Substrate inhibition kinetics. The inset shows the diagnostic EH plot for the same.

one site physically hinders binding to the other site. Substrate inhibition can also occur when the substrate molecule binding to the second binding site causes a change in conformation or efficiency of metabolism at the first binding site. In this scenario, the second binding site is unproductive. One must be careful in interpretation of substrate inhibition in that conditions forced on the system by the inclusion of high substrate concentrations can also cause conformational changes in the enzyme, affect electron transfer, stimulate ionic interactions, or shield ionic interactions, leading to the changes in substrate metabolism rate that mimic true substrate inhibition kinetics. It is unlikely that substrate inhibition will be observed *in vivo* due to the inability to reach the typically high substrate concentrations needed to observe the effect.

The following equation is used to describe data exhibiting substrate inhibition:

$$v = \frac{V_{\max}}{1 + \dfrac{K_{\mathrm{m}}}{[\mathrm{S}]} + \dfrac{[\mathrm{S}]}{K_i}} \tag{9.9}$$

where K_{i} is the inhibition constant of the binding of the second molecule causing the inhibition. One should be careful to not confusion substrate inhibition with product inhibition, which can result in a similar kinetic profile. To do so, one must consider the amount of product formed and the inhibition constant for the product toward the reaction. In general, substrate inhibition is much more common than product inhibition.

9.5.5 Partial Inhibition

Partial inhibition occurs when saturating concentrations of an inhibitor are unable to completely inhibit metabolism of a substrate [70]. This phenomenon is usually indicative of mixed inhibition, wherein a productive enzyme-substrate-inhibitor complex is formed. This complex can continue to form product, hence accounting for the partial inhibition. The inhibitor can either bind to the protein in an allosteric site or in the catalytic pocket of the enzyme, resulting in either conformational changes or steric hindrance, thus affecting the binding and metabolism of the substrate.

9.5.6 Substrate-Dependent Inhibition

Because of the presence of multiple binding sites within an enzyme active site, the potential exists for two molecules that are substrates for the same enzyme to bind to the enzyme but not result in either inhibition or activation. This can result in substrate-dependent inhibition, wherein an inhibitor will inhibit the metabolism of one substrate for the enzyme (i.e., both inhibitor and substrate bind to the same site) but not inhibit the metabolism of another substrate for the same enzyme (i.e., the substrate and inhibitor bind to different sites within the enzyme active site). This is particularly problematic during *in vitro* assessment of drug interactions using a probe substrate. One may miss additional potential interactions with an enzyme when only a single probe substrate is used. In these cases (especially CYP3A4), one should employ at least two probe substrates that are thought to bind to different sites within the active site to best assure assessment of full interaction potential. Substrate-dependent inhibition has been observed for CYP2C9, CYP3A4, and CYP2D6, where K_i values have been found to differ by orders of magnitude depending on the substrate [82–85]. Recently, substrate-dependent inhibition of CYP2D6 was demonstrated, while also suggesting the occurrence of two-site inhibition, such as noncompetitive and uncompetitive inhibition. The observation of both noncompetitive and uncompetitive inhibition further substantiates the possibility that CYP active sites are large enough to accommodate multiple substrates simultaneously.

At least one instance of substrate-dependent inhibition *in vivo* has been reported [86]. Mibefradil (CYP3A4 substrate) coadministration increased triazolam area under the curve (AUC) ninefold, but isradipine (another CYP3A4 substrate) coadministration had a minimal effect on triazolam AUC. Hence, although all mibefradil, isradipine, and triazolam are substrates of CYP3A4, only mibefradil had an effect on triazolam disposition, demonstrating the occurrence of substrate-dependent inhibition in humans.

9.6 *IN VITRO–IN VIVO* CORRELATIONS

An important objective of drug discovery research is the determination of rate of removal of drug *in vivo* and the residence time of the drug in the body. The process of scaling up from *in vitro* systems to *in vivo* systems, commonly referred to as *IVIVCs*, was first developed by Rane *et al*. [87] and further refined by Houston [88] and later Obach *et al*. [65]. The clearance rate of a drug determines its rate of removal from the body. Clearance is defined as the volume of blood cleared of drug per unit time per unit body weight and includes drug removal mechanisms from the gut, liver, kidney, and other organs. To allow direct comparisons between the *in vitro* and *in vivo* situations, one typically estimates the intrinsic clearance (Cl'_{int}), which is the capacity to clear drug from blood in the absence of protein binding and blood flow restrictions. Intrinsic clearance (Eq. 9.10) has the units of the rate of removal of drug per unit concentration:

$$Cl'_{int} = \frac{v}{[S]} \tag{9.10}$$

As described previously, the Michaelis–Menten equation (Eq. 9.1) can be used to fit data that conform to a hyperbolic profile.

In vivo, the concentrations of substrate in the blood rarely approach K_m, such that the [S] in the denominator can be eliminated and Equation 9.1 simplifies to the following:

$$v = \frac{V_{max} \cdot [S]}{K_m} \tag{9.11}$$

Rearranging Equation 9.11 to place [S] on the left-hand side of the equation makes it clear that the following equalities exist:

$$Cl'_{int} = \frac{v}{[S]} = \frac{V_{max}}{K_m} \tag{9.12}$$

Such that the V_{max}/K_m determined from *in vitro* work serves as an approximation of Cl'_{int}, which can be related to the *in vivo* Cl'_{int}. As discussed above, this is predicated on the assumptions that there are no blood flow restrictions, rate is proportional to concentration, that is, the substrate concentrations are in the linear portion of the Michaelis–Menten equation, and there is no protein binding.

If multiple metabolites are formed, the velocities for the formation of all metabolites can be subsequently summed up to determine total intrinsic clearance:

$$Cl'_{int} = \sum \frac{V_{max}}{K_m} \tag{9.13}$$

Early in drug discovery, the metabolic pathway(s) of drug removal has typically not been defined. In this case, the method of substrate depletion (see above) to determine half-life can also be applied to determine intrinsic clearances [65]. Since clearance is also defined as the rate of drug removal per unit time, it is analogous to the first-order rate constant ($k_{elimination}$). Assuming first-order linear kinetics, clearance is equal to the slope obtained from a velocity–substrate plot and can be related to half-life using the following equation:

$$Cl'_{int} = k_{elimination} = \left(\frac{0.693}{\textit{in vitro } t_{1/2}}\right)\left(\frac{\text{mL incubation}}{\text{mg microsomes}}\right) \tag{9.14}$$

The clearance thus obtained is in units of mL/min/mg of microsomal protein. The substrate depletion method has also been validated to predict K_m [38]. This methodology has the particular advantage that the determination of K_m in this manner does not require knowledge of metabolites and pathway.

The intrinsic clearance, as obtained from above calculations, is then scaled up from microsomal quantities to a whole liver. This requires the use of a scaling factor that considers the typical amount of microsomal protein per gram of liver. Multiple values of microsomal protein per gram of liver have been used, ranging from 21 to 77 mg protein/g liver, although a value of 40 mg/g liver is the most widely used scaling factor [65,89]. A more recent review has advocated for the use of a scaling factor of 32 mg/g liver (29–34.4, 95% confidence interval) [90]. This intrinsic clearance can then be scaled from per gram of liver to an average liver weight per person (Eq. 9.15).

$$Cl'_{int} = \left(\frac{0.693}{\textit{in vitro } t_{1/2}}\right)\left(\frac{\text{mL incubation}}{\text{mg microsomes}}\right)\left(\frac{\text{45-mg microsomes}}{\text{g liver}}\right)\left(\frac{\text{20-g liver}}{\text{kg body weight}}\right) \tag{9.15}$$

where the unit of intrinsic clearance is mL/min/kg.

In vitro incubations can also be performed with hepatocytes and as with microsomes, appropriate scaling factors have been developed. The number of hepatocytes per gram of liver has been reported to be between 99×10^6 cells/g of liver ($74–131 \times 10^6$ cells/g, 95% CI) [90] and 120×10^6 cells/g of liver [65] for use in scaling up to the whole liver. Expressed enzymes can also be used to determine intrinsic clearance, although as previously mentioned, there are disadvantages in using this approach since it might overestimate the contribution of the enzyme. A RAF is necessary to standardize the activity of each P450 isoform to its corresponding microsomal activity, which can then be scaled up [13]:

$$\mathrm{RAF} = \frac{\mathrm{Cl}'_{\mathrm{int-HLM}}}{\mathrm{Cl}'_{\mathrm{int-recP450}}} \tag{9.16}$$

This factor needs to be determined for each isoform in the individual expressed enzyme preps using a specific probe substrate, for example, midazolam for CYP3A4 bufurarol for CYP2D6, phenacetin for CYP1A2, and diclofenac for CYP2C9 [13].

Since drugs can bind nonspecifically to proteins during *in vitro* incubations, it is necessary to account for protein binding in the determination of intrinsic clearances:

$$\mathrm{Cl}'_{\mathrm{int,u,inc}} = \left(\frac{0.693}{f_{\mathrm{u,inc}} \cdot t_{1/2}}\right)\left(\frac{\mathrm{mL\ incubation}}{\mathrm{mg\ microsomes}}\right)\left(\frac{\mathrm{45\text{-}mg\ microsomes}}{\mathrm{g\ liver}}\right)\left(\frac{\mathrm{20\text{-}g\ liver}}{\mathrm{kg\ body\ weight}}\right) \tag{9.17}$$

where $f_{\mathrm{u,inc}}$ is the fraction unbound drug in microsomes. When $V_{\max}/K_{\mathrm{m}}$ values are used to calculate intrinsic clearance, only the values of K_{m} need to be adjusted ($f^*_{\mathrm{u,inc}}$ K_{m}) since $V_{\max}$ values will be unaffected. Hepatic clearance ($\mathrm{Cl_H}$) can then be estimated from intrinsic clearance using a hepatic model, such as the well-stirred model [91].

The equation for hepatic clearance using the well-stirred model is as follows:

$$\mathrm{Cl_H} = \frac{Q \cdot \mathrm{Cl_{int}}}{Q + \mathrm{Cl_{int}}} \tag{9.18}$$

where Q is the blood flow to the liver estimated at 20 mL/min/kg for humans.

Incorporating both blood binding and protein binding of the drug, the equation takes the following form [13]:

$$\mathrm{Cl_H} = \frac{Q \cdot f_{\mathrm{u}} \dfrac{\mathrm{Cl}'_{\mathrm{int}}}{f_{\mathrm{u(microsome)}}}}{Q + f_{\mathrm{u}} \dfrac{\mathrm{Cl}'_{\mathrm{int}}}{f_{\mathrm{u(microsome)}}}} \tag{9.19}$$

where f_{u} is the free fraction of the drug in blood and $f_{\mathrm{u(microsome)}}$ is the free fraction in microsomes. Initial studies suggested that blood and microsomal binding may cancel each other out, but several subsequent studies have shown that the free concentration of the drug needs to be utilized in all clearance estimates [92]. A suite of 29 acidic, basic, and neutral compounds were tested for protein binding, and basic compounds exhibited

the greatest microsomal binding as compared with acidic and neutral compounds. In addition, for all compounds, inclusion of both plasma and microsomal binding resulted in the most accurate scale-up estimates [38]. Two reports have provided methodologies to empirically estimate protein binding of drugs in either microsomes or hepatocytes, providing an alternative to experimentally determining protein binding for each drug candidate [93,94].

These estimates of hepatic clearance are made using the assumption that the concentration of drug in the blood is equal to the concentration in the plasma. However, if the blood to plasma concentration ratio of the drug is different from unity, a correction needs to be included [65]:

$$\mathrm{Cl_{bl}} = \frac{\mathrm{Cl_p}}{\mathrm{B/P}} \tag{9.20}$$

where $\mathrm{Cl_{bl}}$ is the blood clearance and B/P the blood to plasma concentration ratio of the drug.

It should be realized that the liver may not be the only organ responsible for clearing the drug. In this case, to determine the total clearance of the drug, one must sum (Eq. 9.21) the clearances from all organs involved in the clearance of the drug from the body, for example, excretory clearance from the kidneys and gut metabolism, though estimation of these individual clearances may not be straightforward:

$$\mathrm{Cl} = \mathrm{Cl_{hepatic}} + \mathrm{Cl_{renal}} + \mathrm{Cl_{intestine}} + \mathrm{Cl_{pulmonary}} + \cdots \tag{9.21}$$

Multiple studies have attempted to use the above IVIVC approach to evaluate the accuracy of predicting the hepatic clearance of a variety of drugs [64,65,92, 95–99]. In general, both microsomes and hepatocytes (fresh and cryopreserved) perform reasonably well in estimating *in vivo* clearance, although all systems tend to underpredict the clearance. Additionally, fresh and cryopreserved hepatocytes were equally proficient in generating clearance estimates for use in predicting *in vivo* clearance when both protein and plasma binding were considered.

9.7 CONCLUDING REMARKS

Determination of *in vitro* enzyme kinetics is critical to drug discovery and drug development. Utilization of the appropriate system and appropriate equations are important to avoid the generation of inaccurate estimates. Several *in vitro* systems (e.g., microsomes, hepatocytes, and expressed enzymes) can be used for this purpose. One must be cognizant of the potential for atypical kinetics and use appropriate kinetic models. When conducted properly, accurate estimates of *in vitro* kinetics can be used to successfully predict the pharmacokinetic properties of drugs, *in vivo*.

ABBREVIATIONS

AUC	Area under the Curve
b5	Cytochrome b_5

CPR	Cytochrome P450 Reductase
DMSO	Dimethyl Sulfoxide
FMOs	Flavin Monooxygenases
HLC	Human Liver Cytosol
HLMs	Human Liver Microsomes
IVIVC	*In vitro–In Vivo* Correlations
NADPH	Nicotinamide Adenine Dinucleotide Phosphate
P450s	Cytochrome P450
PgP	P-Glycoprotein
RAF	Relative Activity Factor
SULTs	Sulfotransferases
UGTs	Glucuronosyltransferase

REFERENCES

1. Caldwell GW. Compound optimization in early-and late-phase drug discovery: acceptable pharmacokinetic properties utilizing combined physicochemical, in vitro and in vivo screens. Curr Opin Drug Discov Devel 2000;3(1):30–41.
2. Raucy JL, Lasker JM. Isolation of P450 enzymes from human liver. Methods Enzymol 1991;206:577–587.
3. Pearce RE, McIntyre CJ, Madan A, *et al*. Effects of freezing, thawing, and storing human liver microsomes on cytochrome P450 activity. Arch Biochem Biophys 1996; 331(2):145–169.
4. Yamazaki H, Inoue K, Turvy CG, *et al*. Effects of freezing, thawing, and storage of human liver samples on the microsomal contents and activities of cytochrome p450 enzymes. Drug Metab Dispos 1997;25(2):168–174.
5. Parkinson A, Mudra DR, Johnson C, *et al*. The effects of gender, age, ethnicity, and liver cirrhosis on cytochrome P450 enzyme activity in human liver microsomes and inducibility in cultured human hepatocytes. Toxicol Appl Pharmacol 2004;199(3):193–209.
6. Soars MG, McGinnity DF, Grime K, *et al*. The pivotal role of hepatocytes in drug discovery. Chem Biol Interact 2007;168:2–15.
7. Oleson L, Court MH. Effect of the beta-glucuronidase inhibitor saccharolactone on glucuronidation by human tissue microsomes and recombinant UDP-glucuronosyltransferases. J Pharm Pharmacol 2008;60(9):1175–1182.
8. Asseffa A, Smith SJ, Nagata K, *et al*. Novel exogenous heme-dependent expression of mammalian cytochrome P450 using baculovirus. Arch Biochem Biophys 1989;274(2): 481–490.
9. Crespi CL, Miller VP. The use of heterologously expressed drug metabolizing enzymes—state of the art and prospects for the future. Pharmacol Ther 1999;84(2): 121–131.
10. Ong CE, Miners JO, Birkett DJ, *et al*. Baculovirus-mediated expression of cytochrome P4502C8 and human NADPH-cytochrome P450 reductase: optimization of protein expression. Xenobiotica 1998;28(2):137–152.
11. Chen L, Buters JT, Hardwick JP, *et al*. Coexpression of cytochrome P4502A6 and human NADPH-P450 oxidoreductase in the baculovirus system. Drug Metab Dispos 1997;25(4):399–405.
12. van Waterschoot RA, van Herwaarden AE, Lagas JS, *et al*. Midazolam metabolism in cytochrome P450 3A knockout mice can be attributed to up-regulated CYP2C enzymes. Mol Pharmacol 2008;73(3):1029–1036.

13. Stringer RA, Strain-Damerell C, Nicklin P, *et al*. Evaluation of recombinant cytochrome P450 enzymes as an in vitro system for metabolic clearance predictions. Drug Metab Dispos 2009;37(5):1025–1034.
14. Subramanian M, Low M, Locuson CW, *et al*. CYP2D6-CYP2C9 protein-protein interactions and isoform-selective effects on substrate binding and catalysis. Drug Metab Dispos 2009;37(8):1682–1689.
15. Subramanian M, Tam H, Zheng H, *et al*. CYP2C9-CYP3A4 protein-protein interactions: role of the hydrophobic N terminus. Drug Metab Dispos 2010;38(6):1003–1009.
16. Gomez-Lechon MJ, Donato MT, Castell JV, *et al*. Human hepatocytes in primary culture: the choice to investigate drug metabolism in man. Curr Drug Metab 2004;5(5):443–462.
17. Li AP, Maurel P, Gomez-Lechon MJ, *et al*. Preclinical evaluation of drug-drug interaction potential: present status of the application of primary human hepatocytes in the evaluation of cytochrome P450 induction. Chem Biol Interact 1997;107(1–2):5–16.
18. Hewitt NJ, Lechon MJ, Houston JB, *et al*. Primary hepatocytes: current understanding of the regulation of metabolic enzymes and transporter proteins, and pharmaceutical practice for the use of hepatocytes in metabolism, enzyme induction, transporter, clearance, and hepatotoxicity studies. Drug Metab Rev 2007;39(1):159–234.
19. Wilkening S, Bader A. Influence of culture time on the expression of drug-metabolizing enzymes in primary human hepatocytes and hepatoma cell line HepG2. J Biochem Mol Toxicol 2003;17(4):207–213.
20. Binda D, Lasserre-Bigot D, Bonet A, *et al*. Time course of cytochromes P450 decline during rat hepatocyte isolation and culture: effect of L-NAME. Toxicol In vitro 2003;17(1):59–67.
21. Guillouzo A, Morel F, Fardel O, *et al*. Use of human hepatocyte cultures for drug metabolism studies. Toxicology 1993;82(1–3):209–219.
22. Cross DM, Bayliss MK. A commentary on the use of hepatocytes in drug metabolism studies during drug discovery and development. Drug Metab Rev 2000;32(2):219–240.
23. McGinnity DF, Soars MG, Urbanowicz RA, *et al*. Evaluation of fresh and cryopreserved hepatocytes as in vitro drug metabolism tools for the prediction of metabolic clearance. Drug Metab Dispos 2004;32(11):1247–1253.
24. Roymans D, Annaert P, Van HJ, *et al*. Expression and induction potential of cytochromes P450 in human cryopreserved hepatocytes. Drug Metab Dispos 2005;33(7):1004–1016.
25. Hutzler JM, Yang YS, Albaugh D, *et al*. Characterization of aldehyde oxidase enzyme activity in cryopreserved human hepatocytes. Drug Metab Dispos 2011;40(2):267–275.
26. Lerche-Langrand C, Toutain HJ. Precision-cut liver slices: characteristics and use for in vitro pharmaco-toxicology. Toxicology 2000;153(1–3):221–253.
27. Edwards RJ, Price RJ, Watts PS, *et al*. Induction of cytochrome P450 enzymes in cultured precision-cut human liver slices. Drug Metab Dispos 2003;31(3):282–288.
28. Vickers AE, Fisher RL. Organ slices for the evaluation of human drug toxicity. Chem Biol Interact 2004;150(1):87–96.
29. Brandon EF, Raap CD, Meijerman I, *et al*. An update on in vitro test methods in human hepatic drug biotransformation research: pros and cons. Toxicol Appl Pharmacol 2003;189(3):233–246.
30. Zientek M, Jiang Y, Youdim K, *et al*. In vitro–in vivo correlation for intrinsic clearance for drugs metabolized by human aldehyde oxidase. Drug Metab Dispos 2010;38(8):1322–1327.
31. Gripon P, Rumin S, Urban S, *et al*. Infection of a human hepatoma cell line by hepatitis B virus. Proc Natl Acad Sci U S A 2002;99(24):15655–15660.
32. Cerec V, Glaise D, Garnier D, *et al*. Transdifferentiation of hepatocyte-like cells from the human hepatoma HepaRG cell line through bipotent progenitor. Hepatology 2007;45(4):957–967.
33. Aninat C, Piton A, Glaise D, *et al*. Expression of cytochromes P450, conjugating enzymes and nuclear receptors in human hepatoma HepaRG cells. Drug Metab Dispos 2006;34(1):75–83.

34. Guillouzo A, Corlu A, Aninat C, *et al*. The human hepatoma HepaRG cells: a highly differentiated model for studies of liver metabolism and toxicity of xenobiotics. Chem Biol Interact 2007;168(1):66–73.
35. Le Vee M, Jigorel E, Glaise D, *et al*. Functional expression of sinusoidal and canalicular hepatic drug transporters in the differentiated human hepatoma HepaRG cell line. Eur J Pharm Sci 2006;28(1–2):109–117.
36. Parent R, Beretta L. Translational control plays a prominent role in the hepatocytic differentiation of HepaRG liver progenitor cells. Genome Biol 2008;9(1):R19.
37. Segel IH. Rapid equilibrium bireactant and terreactant systems. New York: John Wiley and Sons; 1975.
38. Obach RS, Reed-Hagen AE. Measurement of Michaelis constants for cytochrome P450-mediated biotransformation reactions using a substrate depletion approach. Drug Metab Dispos 2002;30(7):831–837.
39. Nath A, Atkins WM. A theoretical validation of the substrate depletion approach to determining kinetic parameters. Drug Metab Dispos 2006;34(9):1433–1435.
40. Kiang TK, Ensom MH, Chang TK. UDP-glucuronosyltransferases and clinical drug-drug interactions. Pharmacol Ther 2005;106(1):97–132.
41. Ohmi N, Yoshida H, Endo H, *et al*. S-oxidation of S-methyl-esonarimod by flavin-containing monooxygenases in human liver microsomes. Xenobiotica 2003;33(12):1221–1231.
42. Lee SK, Kang MJ, Jin C, *et al*. Flavin-containing monooxygenase 1-catalysed N,N-dimethylamphetamine N-oxidation. Xenobiotica 2009;39(9):680–686.
43. Lang DH, Rettie AE. In vitro evaluation of potential in vivo probes for human flavin-containing monooxygenase (FMO): metabolism of benzydamine and caffeine by FMO and P450 isoforms. Br J Clin Pharmacol 2000;50(4):311–314.
44. Stormer E, Roots I, Brockmoller J. Benzydamine N-oxidation as an index reaction reflecting FMO activity in human liver microsomes and impact of FMO3 polymorphisms on enzyme activity. Br J Clin Pharmacol 2000;50(6):553–561.
45. Brockmoller J, Cascorbi I, Kerb R, *et al*. Combined analysis of inherited polymorphisms in arylamine N-acetyltransferase 2, glutathione S-transferases M1 and T1, microsomal epoxide hydrolase, and cytochrome P450 enzymes as modulators of bladder cancer risk. Cancer Res 1996;56(17):3915–3925.
46. Pike MG, Mays DC, Macomber DW, *et al*. Metabolism of a disulfiram metabolite, S-methyl N,N-diethyldithiocarbamate, by flavin monooxygenase in human renal microsomes. Drug Metab Dispos 2001;29(2):127–132.
47. Lang DH, Yeung CK, Peter RM, *et al*. Isoform specificity of trimethylamine N-oxygenation by human flavin containing monooxygenase (FMO) and P450 enzymes - Selective catalysis by FMO3. Biochem Pharmacol 1998;56(8):1005–1012.
48. Hamman MA, Haehner-Daniels BD, Wrighton SA, *et al*. Stereoselective sulfoxidation of sulindac sulfide by flavin-containing monooxygenases. Comparison of human liver and kidney microsomes and mammalian enzymes. Biochem Pharmacol 2000;60(1):7–17.
49. Rawden HC, Kokwaro GO, Ward SA, *et al*. Relative contribution of cytochromes P-450 and flavin-containing monoxygenases to the metabolism of albendazole by human liver microsomes. Br J Clin Pharmacol 2000;49(4):313–322.
50. Sanoh S, Nozaki K, Murai H, *et al*. Prediction of human metabolism of FK3453 by aldehyde oxidase using chimeric mice transplanted with human or rat hepatocytes. Drug Metab Dispos 2012;40(1):76–82.
51. Parkinson A, Ogilvie BW. Biotransformation of xenobiotics. In: Klaassen CD, editor. Casarett and doull's toxicology: the basic science of poisons. 7th ed. New York: McGraw-Hill; 2007. pp. 161–304.
52. Dalvie D, Zhang C, Chen W, *et al*. Cross-species comparison of the metabolism and excretion of zoniporide: contribution of aldehyde oxidase to interspecies differences. Drug Metab Dispos 2010;38(4):641–654.

53. Clarke SE, Harrell AW, Chenery RJ. Role of aldehyde oxidase in the in vitro conversion of famciclovir to penciclovir in human liver. Drug Metab Dispos 1995;23(2):251–254.
54. Barr JT, Jones JP. Inhibition of human liver aldehyde oxidase: implications for potential drug-drug interactions. Drug Metab Dispos 2011;39(12):2381–2386.
55. Alfaro JF, Joswig-Jones CA, Ouyang W, *et al*. Purification and mechanism of human aldehyde oxidase expressed in *Escherichia coli*. Drug Metab Dispos 2009;37(12):2393–2398.
56. Vaidyanathan JB, Walle T. Glucuronidation and sulfation of the tea flavonoid (-)-epicatechin by the human and rat enzymes. Drug Metab Dispos 2002;30(8):897–903.
57. Wang L, Raghavan N, He K, *et al*. Sulfation of o-demethyl apixaban: enzyme identification and species comparison. Drug Metab Dispos 2009;37(4):802–808.
58. Senggunprai L, Yoshinari K, Yamazoe Y. Selective role of sulfotransferase 2A1 (SULT2A1) in the N-sulfoconjugation of quinolone drugs in humans. Drug Metab Dispos 2009;37(8):1711–1717.
59. Miksits M, Sulyok M, Schuhmacher R, *et al*. In-vitro sulfation of piceatannol by human liver cytosol and recombinant sulfotransferases. J Pharm Pharmacol 2009;61(2):185–191.
60. Huang C, Chen Y, Zhou T, *et al*. Sulfation of dietary flavonoids by human sulfotransferases. Xenobiotica 2009;39(4):312–322.
61. Nakano H, Ogura K, Takahashi E, *et al*. Regioselective monosulfation and disulfation of the phytoestrogens daidzein and genistein by human liver sulfotransferases. Drug Metab Pharmacokinet 2004;19(3):216–226.
62. Thomas NL, Coughtrie MW. Sulfation of apomorphine by human sulfotransferases: evidence of a major role for the polymorphic phenol sulfotransferase, SULT1A1. Xenobiotica 2003;33(11):1139–1148.
63. Ung D, Nagar S. Variable sulfation of dietary polyphenols by recombinant human sulfotransferase (SULT) 1A1 genetic variants and SULT1E1. Drug Metab Dispos 2007;35(5):740–746.
64. Jones HM, Houston JB. Substrate depletion approach for determining in vitro metabolic clearance: time dependencies in hepatocyte and microsomal incubations. Drug Metab Dispos 2004;32(9):973–982.
65. Obach RS, Baxter JG, Liston TE, *et al*. The prediction of human pharmacokinetic parameters from preclinical and in vitro metabolism data. J Pharmacol ExpTher 1997;283(1):46–58.
66. Busby WF Jr, Ackermann JM, Crespi CL. Effect of methanol, ethanol, dimethyl sulfoxide, and acetonitrile on in vitro activities of cDNA-expressed human cytochromes P-450. Drug Metab Dispos 1999;27(2):246–249.
67. Korzekwa KR, Krishnamachary N, Shou M, *et al*. Evaluation of atypical cytochrome P450 kinetics with two-substrate models: evidence that multiple substrates can simultaneously bind to cytochrome P450 active sites. Biochemistry 1998;37(12):4137–4147.
68. Atkins WM, Wang RW, Lu AY. Allosteric behavior in cytochrome p450-dependent in vitro drug-drug interactions: a prospective based on conformational dynamics. Chem Res Toxicol 2001;14(4):338–347.
69. Hutzler JM, Tracy TS. Atypical kinetic profiles in drug metabolism reactions. Drug Metab Dispos 2002;30(4):355–362.
70. Tracy TS. Atypical enzyme kinetics: their effect on in vitro–in vivo pharmacokinetic predictions and drug interactions. Curr Drug Metab 2003;4(5):341–346.
71. Tracy TS, Hummel MA. Modeling kinetic data from in vitro drug metabolism enzyme experiments. Drug Metab Rev 2004;36(2):231–242.
72. Tracy TS. Atypical cytochrome P450 kinetics: implications for drug discovery. Drugs R D 2006;7(6):349–363.
73. Subramanian MA, Timothy TS. Allosteric enzyme- and transporter-based interactions. In: Pang S, Rodrigues D, Peter R, editors. Enzyme-and transporter-based drug-drug interactions, New York: Springer; 2010. pp. 497–517.

74. Shou M, Grogan J, Mancewicz JA, *et al*. Activation of CYP3A4: Evidence for the simultaneous binding of two substrates in a cytochrome P450 active site. Biochemistry 1994;33(21):6450–6455.
75. Williams PA, Cosme J, Vinkovic DM, *et al*. Crystal structures of human cytochrome P450 3A4 bound to metyrapone and progesterone. Science 2004;305(5684):683–686.
76. Houston JB, Galetin A. Modelling atypical CYP3A4 kinetics: principles and pragmatism. Arch Biochem Biophys 2005;433(2):351–360.
77. Ngui JS, Tang W, Stearns RA, *et al*. Cytochrome P450 3A4-mediated interaction of diclofenac and quinidine. Drug Metab Dispos 2000;28(9):1043–1050.
78. Tang W, Stearns RA, Kwei GY, *et al*. Interaction of diclofenac and quinidine in monkeys: stimulation of diclofenac metabolism. J Pharmacol Exp Ther 1999;291(3):1068–1074.
79. Hutzler JM, Frye RF, Korzekwa KR, *et al*. Minimal in vivo activation of CYP2C9-mediated flurbiprofen metabolism by dapsone. Eur J Pharm Sci 2001;14(1):47–52.
80. Egnell AC, Houston B, Boyer S. In vivo CYP3A4 heteroactivation is a possible mechanism for the drug interaction between felbamate and carbamazepine. J Pharmacol Exp Ther 2003;305(3):1251–1262.
81. Woods CM, Fernandez C, Kunze KL, *et al*. Allosteric activation of cytochrome P450 3A4 by alpha-naphthoflavone: branch point regulation revealed by isotope dilution analysis. Biochemistry 2011;50(46):10041–10051.
82. Kumar V, Wahlstrom JL, Rock DA, *et al*. CYP2C9 inhibition: impact of probe selection and pharmacogenetics on in vitro inhibition profiles. Drug Metab Dispos 2006;34(12):1966–1975.
83. Stresser DM, Blanchard AP, Turner SD, *et al*. Substrate-dependent modulation of CYP3A4 catalytic activity: analysis of 27 test compounds with four fluorometric substrates. Drug Metab Dispos 2000;28(12):1440–1448.
84. Wang RW, Newton DJ, Liu N, *et al*. Human cytochrome P-450 3A4: in vitro drug-drug interaction patterns are substrate-dependent. Drug Metab Dispos 2000;28(3):360–366.
85. Ramamoorthy Y, Tyndale RF, Sellers EM. Cytochrome P450 2D6.1 and cytochrome P450 2D6.10 differ in catalytic activity for multiple substrates. Pharmacogenetics 2001;11(6):477–487.
86. Backman JT, Wang JS, Wen X, *et al*. Mibefradil but not isradipine substantially elevates the plasma concentrations of the CYP3A4 substrate triazolam. Clin Pharmacol Ther 1999;66(4):401–407.
87. Rane A, Wilkinson GR, Shand DG. Prediction of hepatic extraction ratio from in vitro measurement of intrinsic clearance. J Pharmacol Exp Ther 1977;200(2):420–424.
88. Houston JB. Utility of in vitro drug metabolism data in predicting in vivo metabolic clearance. Biochem Pharmacol 1994;47(9):1469–1479.
89. Hakooz N, Ito K, Rawden H, *et al*. Determination of a human hepatic microsomal scaling factor for predicting in vivo drug clearance. Pharm Res 2006;23(3):533–539.
90. Barter ZE, Bayliss MK, Beaune PH, *et al*. Scaling factors for the extrapolation of in vivo metabolic drug clearance from in vitro data: reaching a consensus on values of human microsomal protein and hepatocellularity per gram of liver. Curr Drug Metab 2007;8(1):33–45.
91. Wilkinson GR, Shand DG. Commentary: a physiological approach to hepatic drug clearance. Clin Pharmacol Ther 1975;18(4):377–390.
92. Riley RJ, McGinnity DF, Austin RP. A unified model for predicting human hepatic, metabolic clearance from in vitro intrinsic clearance data in hepatocytes and microsomes. Drug Metab Dispos 2005;33(9):1304–1311.
93. Austin RP, Barton P, Cockroft SL, *et al*. The influence of nonspecific microsomal binding on apparent intrinsic clearance, and its prediction from physicochemical properties. Drug Metab Dispos 2002;30(12):1497–1503.
94. Austin RP, Barton P, Mohmed S, *et al*. The binding of drugs to hepatocytes and its relationship to physicochemical properties. Drug Metab Dispos 2005;33(3):419–425.

95. Obach RS. Nonspecific binding to microsomes: impact on scale-up of in vitro intrinsic clearance to hepatic clearance as assessed through examination of warfarin, imipramine, and propranolol. Drug Metab Dispos 1997;25(12):1359–1369.
96. Obach RS. Prediction of human clearance of twenty-nine drugs from hepatic microsomal intrinsic clearance data: an examination of in vitro half- life approach and nonspecific binding to microsomes. Drug Metab Dispos 1999;27(11):1350–1359.
97. Grime K, Riley RJ. The impact of in vitro binding on in vitro–in vivo extrapolations, projections of metabolic clearance and clinical drug-drug interactions. Curr Drug Metab 2006;7(3):251–264.
98. Ito K, Hallifax D, Obach RS, *et al*. Impact of parallel pathways of drug elimination and multiple cytochrome P450 involvement on drug-drug interactions: CYP2D6 paradigm. Drug Metab Dispos 2005;33(6):837–844. DOI: 10.1124/dmd.104.003715.
99. Hallifax D, Galetin A, Houston JB. Prediction of metabolic clearance using fresh human hepatocytes: comparison with cryopreserved hepatocytes and hepatic microsomes for five benzodiazepines. Xenobiotica 2008;38(4):353–367.